JCTC Journal of Chemical Theory and Computation

Reaction Mechanism of 1,3,5-Trinitro-*s*-triazine (RDX) Deciphered by Density Functional Theory

Matthew J. Swadley and Tonglei Li*

Pharmaceutical Sciences, University of Kentucky, Lexington, Kentucky 40536

Received June 15, 2006

Abstract: 1,3,5-Trinitro-*s*-triazine, or cyclotrimethylene trinitramine, or RDX, is a sensitive, secondary explosive, which has been the subject of a number of studies regarding the sensitivity and mechanism of decomposition in energetic materials. Several initial mechanistic steps have been proposed for RDX decomposition, with no conclusive agreement upon any one as the definitive pathway. Our research utilizes density functional theory (DFT)-based calculations and concepts, particularly the nuclear Fukui function, to analyze the effects of additive/depletive electronic perturbation upon vapor conformers and crystal RDX structures. Since the nuclear Fukui function is a measure of the physical stress that a nucleus encounters upon a change in the electron population, it may provide useful information regarding the role of each atom in unimolecular decomposition. The results illustrate that both homolytic cleavage of N−N bonds and elimination of HONO from RDX exhibit favorability as initial steps in the decomposition of RDX in either phase. The nuclear Fukui function proved a valuable tool for gaining insight into the initial steps of unimolecular reactions.

Introduction

1,3,5-Trinitro-*s*-triazine (RDX) is a highly symmetric, energetic compound often used as a secondary explosive.[1] Its unimolecular decomposition has recently been the subject of many mechanistic and sensitivity studies, as it has served as a model system for energetic molecules.[2] Despite the growing body of work regarding the compound, however, there has been no conclusive agreement to what the initial mechanistic step is for its decomposition.[3]

Past experimental evidence of RDX decomposition has been interpreted into three distinct initial steps, namely concerted fission, N−N homolysis, and HONO elimination (Figure 1). Concerted fission proceeds through the simultaneous breakage of three C−N bonds, separating the RDX molecule into three molecules of CH_2NNO_2.[4,5] N−N homolysis is self-explanatory, proceeding through the even breakage of a N−N bond into nitrogen dioxide radical and remaining RDX amine radical products.[4,6−9] HONO elimination proceeds by simultaneous breakage of N−N and neighboring C−H bonds, along with the formation of an O−H bond, resulting in the formed HONO.[4,6,7,9] One particular research group has performed a variety of experiments regarding the thermal breakdown of crystal RDX and found that the initial stages of the decomposition may actually occur in the gas and liquid states.[6,7,9] Moreover, decomposition mechanisms in the gas and liquid phase were found to differ from that in the crystal. Depending on if the temperature is above or below RDX's melting point, either melted or vaporized molecules are decomposed first, with their byproducts initiating the breakdown of the crystal proper. These reactions appear to occur through multiple pathways, including those initiated by both HONO elimination and N−N homolysis. Many experiments involving the shock or UV photolysis detonation of crystal RDX point to the initial reaction step of N−N homolysis.[8,10−13] One in particular involved the pyrolysis of a thin film of RDX with a pulsed CO_2 laser, yielding N_2O_4, the product of two NO_2 radicals formed from RDX N−N homolysis.[8] Another study dealt with the shock-induced decomposition of crystal RDX and found a decrease in the ratio of nitro-group nitrogen atoms to ring-bound amine nitrogen atoms through X-ray

* Corresponding author phone: (859)257-1472; fax: (859)257-7585; e-mail: tonglei@uky.edu. Corresponding author address: 514 College of Pharmacy, University of Kentucky, 725 Rose Street, Lexington, KY 40536-0082.

10.1021/ct600202e CCC: $37.00
Published on Web 01/06/2007

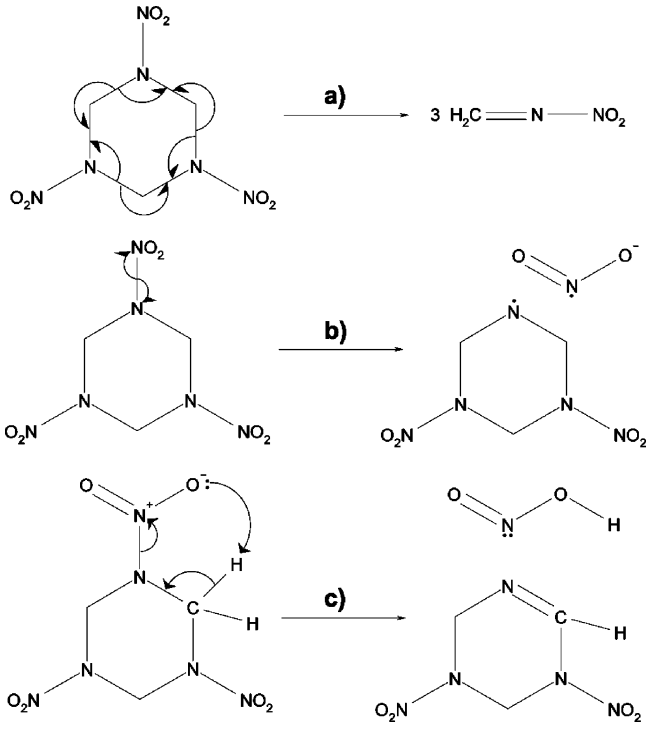

Figure 1. Summary of proposed mechanistic steps for RDX decomposition, concerted fission (a), N−N homolysis (b), and HONO elimination (c).

photoelectron spectroscopy (XPS) after the shock of a sample crystal.[12] This, combined with electron paramagnetic resonance (EPR) evidence of nitro group radical products from the reaction, indicated to the authors that N−N homolysis may indeed be the initial step in mechanically impacted RDX crystals.[12] A study by Chakraborty et al. in which the transition state energies of each decomposition pathway (concerted fission, N−N homolysis, and HONO elimination) were calculated with quantum mechanical methods yielded insight into the mechanistic feasibility of these paths in the gas phase.[4] In this study, it was found that the HONO elimination mechanism was most favorable, with N−N cleavage also having energetic favorability. The concerted fission mechanism, proposed from earlier experimental evidence,[5] was ruled out as an initial step to detonation due to its transition state existing at a much higher energy than the other pathways.

There have been many recent investigations that study the crystal structure of RDX as a means to identify trends in its reactivity. Many of these studies have focused upon the RDX lattice and its role in the ease of electronic excitation (perturbation). Electronic excitation (resulting from shock, heat, or UV energy) is often discussed in terms of narrowing and disappearance of the gap between valence and conduction bands in crystalline solids, which can initiate chemical reactions such as detonation through conformational changes and bond breakage.[14,15] Experimental evidence showing increases in the conductivity of RDX crystals just before detonation support this assertion, as closing of the band gap would allow for free electron movement throughout the compound.[16−19] RDX crystals containing defects have been shown to be more detonation shock-sensitive than perfect crystals.[20] Localized regions of focused energy from shock within a crystal known as "hot spots" have recently been studied.[21−24] These studies have theoretically calculated the narrowing of the valence-conduction band gap of the RDX crystal in the presence of several types of defects (including edge dislocations, vacancies and cracks) at various unit cell volume compressions. It was found that unit cell compression, a product of mechanical shock, and edge dislocations significantly reduce the band gap in RDX crystals.[22−24] Another study analyzed the feasibility of charge-transfer (CT) pair formation in RDX crystals and their relation to detonation sensitivity in perfect and defect-containing crystals.[1] CT pairs are a potential mechanism of electronic perturbation in crystals where an electron from one molecule is transferred to another, resulting in neighboring cationic and anionic molecules.[1] It was found that the energy released from a relaxing CT pair in a crystal containing vacancy defects is enough to break an $N-NO_2$ bond in RDX, potentially inducing detonation. Recently, studies have also been performed to evaluate the mechanical strength of the RDX lattice through its elasticity constants.[25−29] It has been proposed that stiffer lattices imply less sensitive shock detonation in energetic materials, as stiffness rankings in RDX homologues are the reverse of detonation sensitivity.[26]

In a previous study by Luty et al., the nucleophilic and electrophilic nuclear Fukui functions, chemical reactivity index, and nuclear stiffness were calculated to analyze the effects of electronic perturbation upon RDX nuclei.[2] The results yielded novel insight into how the responses of individual nuclei to perturbation can be interpreted with mechanistic implications. It was found that while the geometric structure of an RDX molecule had a C_{3v} symmetric structure, the electronic structure was reduced to C_s symmetry upon electronic perturbation, evidenced by asymmetric chemical reactivity index and nuclear stiffness magnitudes on symmetrically similar nitrogen atoms. These asymmetrical responses focused strain resulting from electronic perturbation on a particular set of bonded nitrogen atoms, which were concluded to displace from one another more easily than the others within the molecule. This focused strain was also related to the decomposition sensitivity exhibited by RDX as well as evidence for the N−N homolysis mechanism.

The subject of the previous research by Luty et al. was limited to the triaxial (AAA) conformer of RDX and did not yet account for effects of the crystal electronic structure. Vapor-phase RDX has been shown to exist as a superposition of several conformers, denoted by the nitro group positions (as either axial or equatorial) and ring conformations (as chair, boat, or twist).[4,30−32] The molecular energies of such conformers exist at comparable energies, indicating that a high degree of interconversion is possible.[4,30−32] Previous literature has also shown that the most stable conformers appear to be the chair triaxial (AAA) form and the chair diaxial form (AAE), with energy rankings differing in separate accounts.[4,30−32] Infrared spectra of experimental RDX vapor correlates well with simulated spectra for the triaxial (AAA) conformer, indicating that it may be the best representative of the structure of gaseous RDX.[32] Single-crystal neutron-diffraction, however, has shown crystal RDX has a diaxial (AAE) conformation.[33] Structural differences

between interconverting molecular conformers as well as intermolecular influences from the RDX lattice may imply that more calculations are necessary to better understand gaseous and solid-state perturbation responses in RDX.

Our research seeks to utilize conceptual density functional theory (DFT)-based concepts, most notably the nuclear Fukui function, to shed light on how electronic perturbation can reveal the initial decomposition mechanism of RDX vapor and crystals. Previous investigations from our research group have studied reactivity in crystal systems using conceptual DFT methods, with an emphasis upon reactivity differences in polymorphs of the same compound.[34,35] The nuclear Fukui function has proven to be a key tool for identifying the role of a compound's electronic structure in its reaction mechanism. In one particular study,[35] we compared nuclear Fukui function values of α- and γ-indomethacin, which were experimentally shown to have different reaction rates with ammonia gas, α-form being faster. Upon analysis of the nucleophilic nuclear Fukui function, it was found that a particular set of symmetrically similar indomethacin molecules in the α-form had significantly larger responses upon the reactive carboxylic hydrogen atom than any in the γ-form. This was concluded to be evidence that the electronic structure of the α-form allows easier dissociation of the acidic hydrogen, hence accounting for its greater reactivity. We believe that the insight gained through analysis of nuclear Fukui functions in indomethacin crystals can be applied to better understand the initial decomposition mechanism of RDX.

Methods

The nuclear Fukui function is derived from DFT, which states that electron density is the fundamental quantity for describing atomic and molecular ground states and that energy is a functional of electron density.[36−38] A full derivation of the nuclear Fukui function can be seen in our previous reports.[34,35] In brief, the nuclear Fukui function has its roots in the Hellmann-Feynmann force, denoted as the force upon nucleus α within a molecular system[39,40]

$$\mathbf{F}_\alpha = Z_\alpha \left[\int \rho(\mathbf{r}) \frac{\mathbf{r}_\alpha}{r_\alpha^3} d\mathbf{r} - \sum_{\beta \neq \alpha} Z_\beta \frac{\mathbf{R}_{\alpha\beta}}{R_{\alpha\beta}^3} \right] \quad (1)$$

where $\rho(\mathbf{r})$ is the electron density at point $\mathbf{r}$, $\mathbf{r}_\alpha$ is equal to the displacement vector between the position of nucleus α and point $\mathbf{r}$, and $\mathbf{R}_{\alpha\beta}$ is the displacement vector between nucleus α and nucleus β with their charges as Z_α and Z_β, respectively. It is evident that from this equation $\mathbf{F}_\alpha$ is dependent in part upon the molecular system's electronic structure. The concept of the nuclear Fukui function (Φ_α) is developed from the response of $\mathbf{F}_\alpha$ to a perturbation of the electronic structure, defined as[41]

$$\Phi_\alpha = \left(\frac{\partial \mathbf{F}_\alpha}{\partial N} \right)_\nu \quad (2)$$

where N is the number of electrons in the system and $\nu(\mathbf{r})$ is the external potential defined by nuclear charges, $\{Z_\alpha\}$, and nuclear position vectors, $\{\mathbf{R}_\alpha\}$. Therefore, the nuclear Fukui function characterizes the force that nucleus α experiences upon a change in the electronic number or density due to perturbation or exchange with neighboring systems. Since it is expected that large nuclear Fukui function force responses can identify atomic displacement, they can be used as a means to investigate chemical reactivity. Because N has to be integers, in practice, the smallest change in N is one. As such, the nuclear Fukui function concept can be further developed into nucleophilic and electrophilic components, numerically calculated by the finite differences[41]

$$\Phi^+{}_\alpha = \mathbf{F}^+{}_\alpha - \mathbf{F}^0{}_\alpha$$

$$\Phi^-{}_\alpha = \mathbf{F}^0{}_\alpha - \mathbf{F}^-{}_\alpha \quad (3)$$

where $\Phi^+{}_\alpha$ is the nuclear Fukui function for nucleophilic attack on nucleus α, $\Phi^-{}_\alpha$ is the nuclear Fukui function for electrophilic attack, and $\mathbf{F}^+{}_\alpha$, $\mathbf{F}^-{}_\alpha$, and $\mathbf{F}^0{}_\alpha$ are the Hellman-Feynmann forces on the anionic, cationic, and neutral compound species, respectively. It should be noted that for molecules at equilibrium (in any phase), $\mathbf{F}^0{}_\alpha$ is close to zero, so $\mathbf{F}^+{}_\alpha$ and $\mathbf{F}^-{}_\alpha$ may independently characterize nucleophilic or electrophilic attack, respectively.[42] In the case of unimolecular decomposition, electronic perturbation may occur through the momentary addition or depletion of electron density to/from the molecular structure, so both the nucleophilic and electrophilic nuclear Fukui functions may be useful as a means of assessing reactivity and identifying the initial bond-breaking site(s) in RDX. It should be noted that nuclear Fukui functions of a molecular system are calculated with nucleus positions remaining fixed, while the electronic structure is perturbed. The applicability of these functions for understanding a chemical reaction where old bonds are broken and new ones are formed follows the assumption that changes in the electron density lead to the reorganization of the nuclear geometry.[43]

Single RDX molecules of AAA, AAE, AEE, and EEE conformers were optimized using the program package Gaussian 03 (Gaussian, Inc., Wallingford, CT) at a B3LYP/6-311G(2d,p)++ level of accuracy. In addition the α-form RDX crystal (*Pbca*, $a = 13.182$, $b = 11.574$, $c = 10.709$Å, $\alpha = \beta = \gamma = 90°$, $Z = 8$)[33] was optimized with constant unit cell parameters at a B3YLP/6-21G(d,p) level of accuracy using the Crystal 03 code package.[44] Nuclear Fukui function calculations were made from the optimized structures at the same levels of accuracy. All calculations were performed on a 28-CPU Linux cluster. The magnitudes of crystal RDX nuclear Fukui function values have been normalized by a factor of 8 ($Z = 8$ in the α-RDX crystal unit cell) as a means to enhance comparability of trends within each system. This normalization should not be misconstrued to be useful in the comparison of raw values between single molecules and the crystal structure, as the calculations for each have been performed at different levels of accuracy and have been perturbed in different manners (adding/depleting one electron per molecule vs adding/depleting one electron per volume of the unit cell).

Results and Discussion

Vapor-Phase RDX. As stated earlier, it is believed that vapor-phase RDX exists as a superposition of several

Table 1. Nucleophilic (Φ^+_α) and Electrophilic (Φ^-_α) Nuclear Fukui Function Magnitudes of Vapor-Phase RDX in the Triaxial (AAA), Diaxial (AAE), Diequatorial (AEE), and Triequatorial (EEE) Conformations[a]

	$\lvert\Phi^+_\alpha\rvert$				$\lvert\Phi^-_\alpha\rvert$			
	AAA	AAE	AEE	EEE	AAA	AAE	AEE	EEE
C1	0.6827	0.5939	0.5965	0.6537	1.7682	1.1046	2.7983	2.1930
C2	0.6834	0.6715	0.6066	0.6550	0.7988	2.5481	1.0588	2.1910
C3	0.6831	0.5939	0.6066	0.6540	1.8626	1.1010	1.0608	2.1921
H1	0.1767	0.1827	0.3661	0.4176	0.1543	0.1514	0.2178	0.1242
H2	0.1721	0.1106	0.1048	0.1136	0.1571	0.1649	0.7965	0.4520
H3	0.1740	0.1854	0.1135	0.1138	0.1463	0.1415	0.1937	0.4525
H4	0.1762	0.1088	0.2304	0.4181	0.2462	0.0581	0.2659	0.1246
H5	0.1767	0.1827	0.2303	0.4173	0.1471	0.1518	0.2652	0.1242
H6	0.1723	0.1105	0.1135	0.1137	0.1551	0.1649	0.1925	0.4521
N1	0.8574	0.5112	0.6342	0.7282	2.8836	0.3836	2.1790	2.3179
N2	0.8701	1.0421	0.6340	0.7305	0.8757	2.6350	2.1843	2.3237
N3	0.8654	1.0418	1.2290	0.7341	0.9792	2.6346	1.6068	2.3165
N4	2.2475	2.4715	2.6007	2.6643	4.3974	0.4358	3.5831	4.0688
N5	2.2710	2.5791	2.6002	2.6635	1.3913	4.1012	3.5897	4.0674
N6	2.2664	2.5782	2.8767	2.6709	1.5595	4.1007	3.0082	4.0631
O1	3.0257	2.8081	2.9601	2.9905	1.1426	0.6962	1.2616	1.1550
O2	3.0265	2.8080	3.0166	2.9910	1.1449	0.6972	0.9794	1.1543
O3	3.0560	3.0195	2.9594	2.9799	0.7536	1.0048	1.2624	1.1550
O4	3.0610	3.2731	3.0157	2.9802	0.6190	1.1928	0.9812	1.1540
O5	3.0563	3.0188	3.0623	2.9866	0.7751	1.0048	0.8524	1.1535
O6	3.0606	3.2725	3.0623	2.9864	0.6425	1.1927	0.8526	1.1536

[a] Unit: nN.

conformers.[4,30−32] In order to assess the initial decomposition step in the single RDX molecule, nuclear Fukui functions of each axial−equatorial chair conformation were calculated (Table 1). Energetically, the AAE conformation was found to be most stable, with the AAA and AEE conformations existing at slightly higher energies (about 3.05 and 3.53 kJ/mol higher, respectively). The EEE conformer is less stable, with a total energy 18.87 kJ/mol higher than the AAE conformation. Vapor-phase RDX, therefore, may have a minimal probability of existing in the EEE conformer at any instant in time. These values support the idea that interconversion may exist between at least the AAA, AAE, and AEE conformers in the gas phase.

Several trends can be interpreted from the nuclear Fukui function data (vector representations shown in Figures 2 and 3) as they pertain to the initial mechanistic steps proposed in the literature. First, the data suggest that concerted fission (Figure 1a) is not a likely initial step in RDX vapor. The concerted fission mechanism proceeds through the simultaneous breakage of C−N bonds within the ring of RDX. If this mechanism were likely, the largest nuclear Fukui function values would occur at carbon and ring-bound nitrogen atoms. The nucleophilic nuclear Fukui function magnitudes ($\lvert\Phi^+_\alpha\rvert$) provide no such evidence in any conformation, as the largest values occur in nitro group nitrogen and oxygen atoms. Carbon atoms values (in the range of 0.59−0.69 nN) and ring-bound amine nitrogen atom values (in the range of 0.51−1.23 nN) in general have far smaller response values than these nitro group atoms (nitrogen atoms between 2.24 and 2.88 nN, oxygen atoms between 2.80 and 3.28 nN). This indicates that reactivity

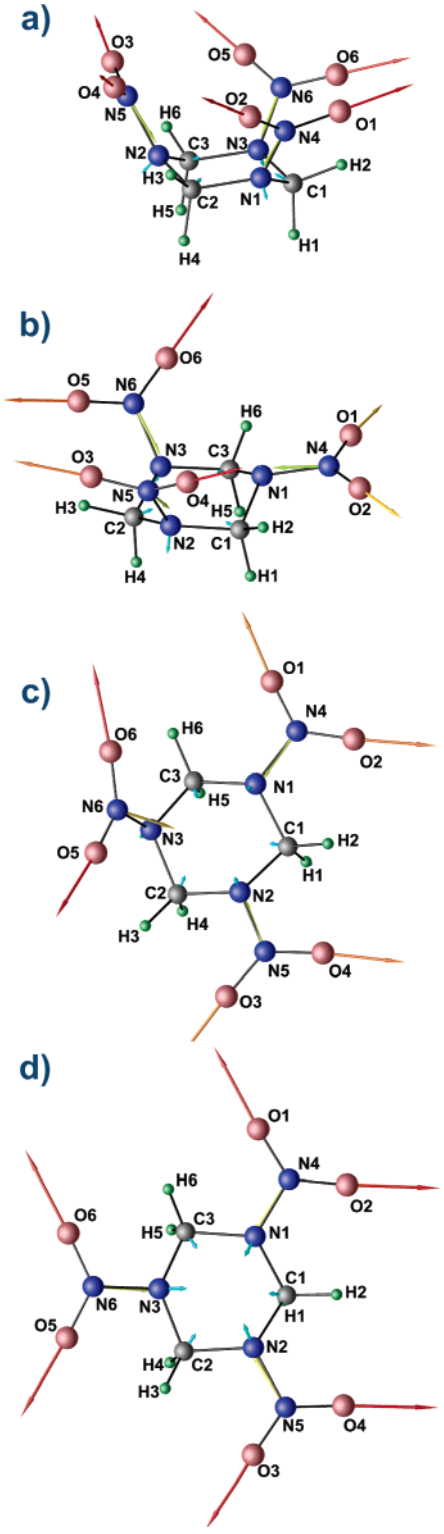

Figure 2. Vector representations of nucleophilic nuclear Fukui functions (Φ^+_α) for single RDX molecules of the AAA (a), AAE (b), AEE (c), and EEE (d) conformers. Vector lengths (small to large) and colors (blue to red) represent relative magnitudes of the nuclear Fukui functions within each particular molecule.

due to the addition of an electron to a single molecule of RDX will tend to involve the nitro groups more than ring-bound carbon and nitrogen atoms. The electrophilic nuclear Fukui function magnitudes ($\lvert\Phi^-_\alpha\rvert$) provide similar evidence, as concerted fission does not appear to be a likely pathway

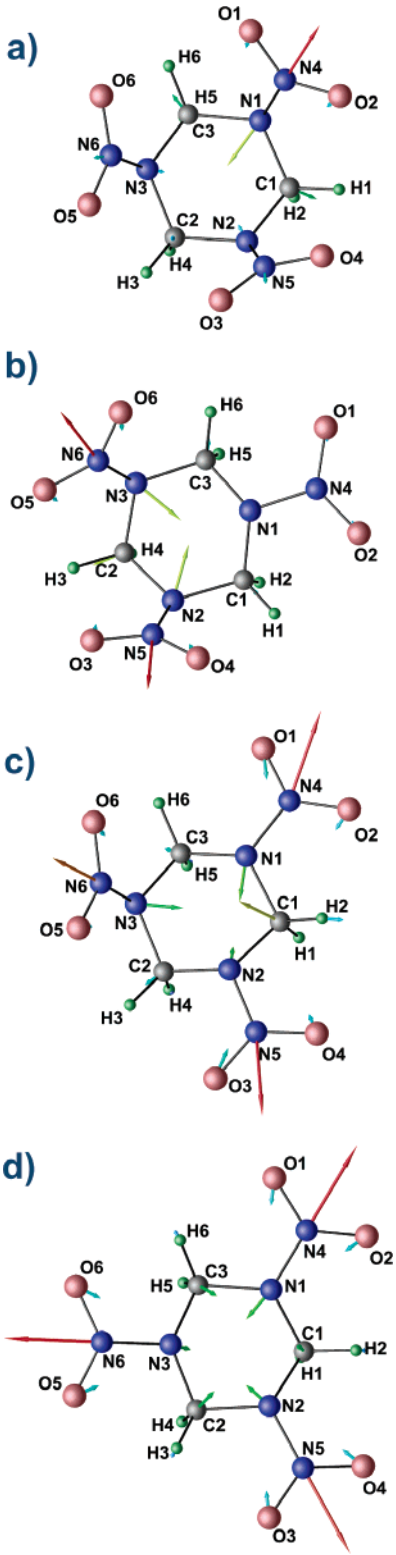

Figure 3. Vector representations of electrophilic nuclear Fukui functions (Φ^-_α) for single RDX molecules of the AAA (a), AAE (b), AEE (c), and EEE (d) conformers. Vector lengths (small to large) and colors (blue to red) represent relative magnitudes of the nuclear Fukui functions within each particular molecule.

for electron depleted systems. The electrophilic carbon and ring-bound nitrogen atom values are larger than their nucleophilic counterparts but are still outweighed in general by values within the nitro groups. In the AAA conformer, the largest four electrophilic nuclear Fukui function forces occur at N4 (4.40 nN), N1 (2.88 nN), C3 (1.86 nN), and C1 (1.77 nN). Even though there are large force responses between the bonded atoms N1−C1 and N1−C3, the most likely mechanistic step would indicate the breakage of the N1−N4 bond in this conformer. The other conformers show similar trends, as even with some carbon atoms having large electrophilic responses, the largest force responses occur at bonded nitrogen regions (N2−N5, N3−N6 in AAE, N1−N4, N2−N5 in AEE, all N−N bonds in EEE). From the Φ^+_α and Φ^-_α magnitudes, it is evident that the concerted fission mechanism is not the most likely initial step in the decomposition of RDX gas.

Both $|\Phi^+_\alpha|$ and $|\Phi^-_\alpha|$ provide evidence that N−N breakage may occur in RDX decomposition. This is evidenced by large nucleophilic responses for nitro group nuclei and strong electrophilic responses upon bonded nitrogen atoms. This breakage is necessary for both the N−N homolysis and HONO elimination mechanisms (Figure 1b,c).[4] HONO elimination requires the additional breakage of a C−H bond accompanied by formation of an O−H bond. Distinguishing these mechanisms from one another may therefore depend upon nuclear Fukui function magnitudes on carbon and hydrogen atoms as well as O−H proximity within each conformer.

In the AAA and AAE conformers, noted from the literature as the most stable conformers,[4,30−32] there is no evidence of a significantly large hydrogen atom electrophilic or nucleophilic force response, as Φ^+_α and Φ^-_α magnitudes are less than 0.25 nN. However, $|\Phi^-_\alpha|$ in the AEE conformer do provide some evidence of HONO elimination. H2 has a Φ^-_α magnitude of 0.7965 nN (about 4 times larger than in the AAA or AAE conformer and at least 3 times larger than any other hydrogen atom in the same conformer) and is bonded to C1, whose magnitude is relatively large at 2.7983 nN. While the H2 force is not as large as those upon other atoms within the molecule, its effect upon displacement of the hydrogen atom may be significant due to hydrogen's small mass. These significantly large C1 and H2 values indicate that bond breakage may occur at this site. Moreover, H2 is in close proximity of O2 and O4, members of nitro groups with significantly large nitrogen Φ^-_α values (N4 and N5). From these data, it certainly seems plausible that HONO elimination of H2−O2−N4−O1 or H2−O4−N5−O3 could occur. In the EEE conformer, HONO elimination seems a possible mechanism as well, with H2, H3 and H6 having larger Φ^-_α values (all about 0.45 nN) paired with carbon atom Φ^-_α values of about 2.2 nN. However, the feasibility of mechanisms in this conformer may be hampered by the large relative energy as compared to conformers with axial nitro groups. In the vapor phase, it seems that the AAA and AAE conformers are more likely to decompose through the N−N homolysis route, while the AEE and EEE conformers seem to exhibit evidence of HONO elimination initiated decomposition.

Symmetry also seems to play a role in the reactivity of compounds. One of the most intriguing findings of previous RDX research was the asymmetric responses of seemingly similar bonded nitrogen atoms found by Luty et al., which would focus perturbation response strain in the AAA

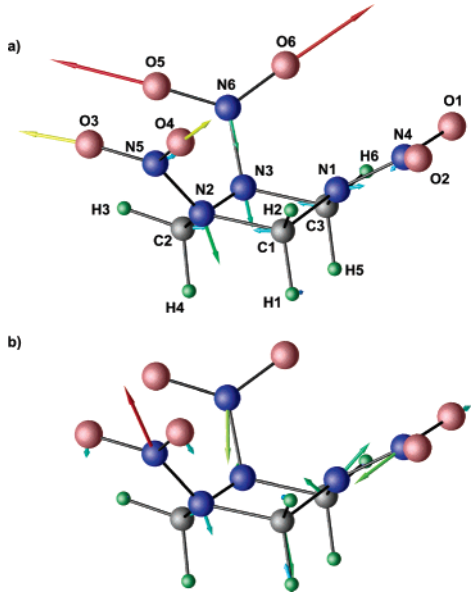

Figure 4. Vector representations of the nucleophilic (a) and electrophilic (b) nuclear Fukui functions for a molecule in crystal RDX. Vector lengths (small to large) and colors (blue to red) represent relative magnitude within the molecule.

conformer onto one bond.[2] Each RDX conformer exhibits structural symmetry, with the AAA and EEE conformers exhibiting C_{3v} symmetry and the AAE and AEE conformers exhibiting C_s symmetry. Their findings for the AAA conformer are echoed in this report, as the electrophilic nuclear Fukui function has far larger magnitudes upon the bonded N1 and N4 atoms than other nitrogen atoms within the same molecule. This indicates that the perturbed electronic structure of AAA RDX does not have the same symmetry as the geometric structure. The shape of the highest occupied molecular orbital (HOMO) of AAA RDX (Figure 5a) further emphasizes this point, as while the molecular structure has C_{3v} symmetry, the orbital is only C_s symmetric. When an electron is removed from a molecule, it is removed from the HOMO, which helps to explain the asymmetric Φ^-_α values.

The electronic symmetries of the other RDX conformers, however, seem to match the symmetries in their skeletal structures. In the EEE conformer, which exhibits structural C_{3v} symmetry, each symmetrically similar atom has similar nuclear Fukui function values (i.e., each carbon, hydrogen, and nitro group experiences similar force responses to additive or depletive electronic perturbation, Figures 2 and 3). In Figure 5g,h, the shapes of the HOMO and LUMO of the EEE conformer exhibit C_{3v} symmetry, illustrating the similar responses for symmetrically similar atoms upon electron addition/depletion. The AAE and AEE skeletal structures have C_s symmetry, with reflection planes defined by C2, N1, and N4 in AAE and C1, N3, and N6 in AEE. Nuclear Fukui function directions and magnitudes show that the symmetries of the electronic structures match those of the skeletal structures in these conformers. In the AAE conformer, similar atoms within the axial nitro groups have similar Φ^+_α and Φ^-_α values, as do C1/C3 and O1/O2. In the AEE conformer, similar atoms within the equatorial nitro groups have similar Φ^+_α and Φ^-_α values, as do C2/C3 and

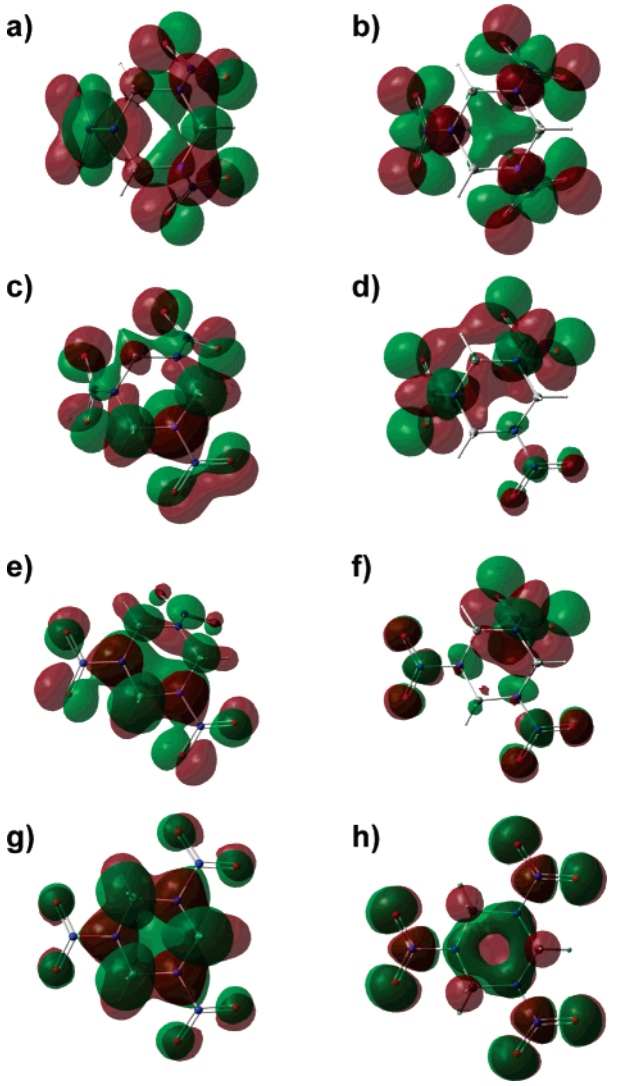

Figure 5. Highest Occupied Molecular Orbital (HOMO) and Lowest Unoccupied Molecular Orbital (LUMO) visualizations for AAA (a, b), AAE (c, d), AEE (e, f), and EEE (g, h) conformers of vapor-phase RDX.

O5/O6. These symmetry trends are also seen in the shapes of the HOMOs and LUMOs (Figure 5c−f).

RDX Crystal. First, the values of the nuclear Fukui functions (Table 2, vector representations in Figure 4) in the α-form RDX crystal do not seem to suggest that concerted fission is a likely initial mechanistic step for decomposition, as initial, simultaneous breakage of C−N bonds seems unlikely. Upon analysis of the nucleophilic nuclear Fukui function (Φ^+_α) magnitudes, it can be seen that the largest values occur at oxygen atoms in the axial positions (O5 > O6 > O3 > O4), followed by N2, N6, and N3 in order of strength. The three carbon atoms follow after these values, with magnitudes of about 1.14−1.18 nN. These data suggest that reactivity as a result of adding an electron to the system would more likely affect axial nitro groups, rather than C−N bonding, not to mention that multiple breakages of C−N bonds are required to generate the CH_2NNO_2 products. The electrophilic nuclear Fukui function (Φ^-_α) magnitudes also preclude concerted fission as a mechanism, as the strongest magnitudes reside on bonded nitrogen pairs, rather than C−N pairs. The largest force magnitudes are upon atoms N5, N6,

Table 2. Nucleophilic (Φ^+_α) and Electrophilic (Φ^-_α) Nuclear Fukui Function Magnitudes for the Vapor-Phase AAE Conformer and α-Crystal[a]

	$\lvert\Phi^+_\alpha\rvert$		$\lvert\Phi^-_\alpha\rvert$	
	vapor	crystal	vapor	crystal
C1	0.5939	1.1849	1.1046	1.2585
C2	0.6715	1.1449	2.5481	0.9331
C3	0.5939	1.1878	1.1010	0.9693
H1	0.1827	0.4386	0.1514	0.4581
H2	0.1106	0.2812	0.1649	0.3895
H3	0.1854	0.2795	0.1415	0.1579
H4	0.1088	0.3329	0.0581	0.1319
H5	0.1827	0.2766	0.1518	0.1795
H6	0.1105	0.2986	0.1649	0.1818
N1	0.5112	1.1229	0.3836	1.0337
N2	1.0421	2.1837	2.6350	0.7651
N3	1.0418	1.6533	2.6346	1.3260
N4	2.4715	0.7777	0.4358	1.4564
N5	2.5791	0.8980	4.1012	2.2703
N6	2.5782	1.8595	4.1007	1.4622
O1	2.8081	0.2897	0.6962	0.7452
O2	2.8080	0.2040	0.6972	0.2171
O3	3.0195	3.1171	1.0048	0.8051
O4	3.2731	3.0391	1.1928	0.7158
O5	3.0188	4.1742	1.0048	0.2396
O6	3.2725	4.1195	1.1927	0.3215

[a] Atom naming corresponds with Figure 4. Unit: nN.

N3, N4, and C1 in order of decreasing magnitude. The bonded C−N pair with the strongest $\lvert\Phi^-_\alpha\rvert$ values, C1−N1, (combined magnitudes of about 2.26 nN) seems less likely to break than does N1−N4 (combined about 2.5 nN), N3−N6 (about 2.79 nN), or N2−N5 (about 3 nN). Also, no other carbon atom has a value large enough to indicate a second C−N breakage that would form the proper CH_2NNO_2 products resulting from the concerted fission mechanism.

Nuclear Fukui function data do seem to indicate that N−N breakage is likely to occur as a result of electronic perturbation in RDX crystals. Upon the addition of electron density to the crystal structure, the largest force responses occur within the axial nitro groups (N6−[O5,O6] and N5−[O3,-O4]) and their connecting ring-bound nitrogen atoms (N2 and N3). Upon depletion of electron density, the largest force responses occur between connected nitrogen atoms (N1−N4, N2−N5, and N3−N6), with axial nitro groups having slightly larger responses. Breakage of the N−N bonds is critical to both the N−N homolysis and HONO elimination mechanisms. As in the RDX vapor conformers, the presence of large nuclear Fukui function responses upon bonded carbon-hydrogen pairs combined with proximity to reactive nitro groups may be used to discriminate HONO elimination over N−N homolysis in the RDX crystal.

The nucleophilic nuclear Fukui function provides only slight evidence of such an interaction. H1 has an asymmetrically large magnitude (0.4386 nN), about 50% larger than the average of the other hydrogen atoms within the crystal (about 0.29 nN). However, H1 does not appear to be in a position to form a bond with an oxygen atom of a reactive axial nitro group, the closest being O4. As seen in Figure 4, H1 is on the opposite side of the ring as O4, making the possibility of bond formation unlikely. This seems to indicate that N−N homolysis is the most likely mechanistic route of decomposition due to additive electron perturbation. The electrophilic nuclear Fukui function shows that both H1 and H2 have significantly larger responses upon removal of an electron than other hydrogens within the crystal. $\lvert\Phi^-_\alpha\rvert$ on H1 (0.4581 nN) is nearly 3 times larger than those on hydrogen atoms not bonded to C1, and H2 (0.3895 nN) is about 2.3 times larger. As seen in Figure 4, H2 is much closer to O4 than H1, indicating that it may be able to form a bond with O4 in the event of perturbation. This seems to indicate that HONO elimination, in addition to N−N homolysis, may be a reaction path in crystal RDX.

The crystal lattice of α-RDX has a profound effect upon the symmetry of the electronic structure of its individual molecules. As shown before, the electronic structure of the HOMO and LUMO in the vapor-phase AAE had the same symmetry as its molecular skeleton, and this fact was reinforced by the magnitudes and directions of the nuclear Fukui functions. Despite their AAE molecular conformation, the electronic structures of RDX crystal molecules seem to be skewed from such a C_s symmetry. Evidence of this is seen throughout the RDX crystal molecule in its nuclear Fukui functions, as symmetrically similar atoms do not have similar magnitudes and directions (Figure 4). The axial nitro groups (N2−N5−[O3, O4] and N3−N6−[O5, O6]) do not have similar values for either the nucleophilic or electrophilic nuclear Fukui function, and the methyl groups that connect each axial nitro group to the equatorial one (C1−[H1, H2] and C3−[H5, H6]) also experience asymmetric responses to depletive electronic perturbation. The asymmetry upon axial bonded nitrogen atoms provides interesting force responses upon perturbation, especially at the N2−N5 bonded region. Upon addition of electron density, N2 has the largest response upon a non-oxygen nucleus within the molecule (2.1837 nN), but its bonded counterpart, N5, has a relatively small value (0.8980 nN). Upon the removal of electron density, however, N5 has the largest response of any nucleus within the molecule (2.2703 nN), while N2's is surprisingly small (0.7651 nN). The other axial bonded nitrogen atoms, N3 and N6, have similar responses upon either type of perturbation. Despite the sums of the responses for each of these bonded pairs being comparable for both the nucleophilic and electrophilic nuclear Fukui functions, it certainly appears that perturbation affects each in a quite different manner.

In summary, we have calculated the optimized structures, energies, and nuclear Fukui functions of RDX AAA, AAE, AEE, and EEE conformations as well as of α-RDX single crystals in an effort to understand the initial step of its unimolecular decomposition. In the vapor phase, RDX showed favorability for both the N−N homolysis and HONO elimination mechanisms. The calculated nuclear Fukui functions for AAA and AAE conformers provided the best support for N−N homolysis, as the largest responses occurred at bonded N−N sites, and no large responses were found on hydrogen atoms within the molecular structure. The AEE and EEE conformers, however, showed that HONO elimination may indeed be a viable reaction path, as strong N−N

force responses were paired with significantly large C−H magnitudes and proper H orientation for O−H formation. Data for the EEE conformer, however, may not be as applicable to the mechanism of vapor-phase RDX breakdown, as its higher energy may indicate that the conformer contributes less to the overall interconverting structure. Moreover, solid α-RDX showed favorability for the N−N homolysis mechanism. This is due to large nucleophilic nuclear Fukui function magnitudes upon atoms in axial $N-NO_2$ groups and strong electrophilic N−N responses. There was also some evidence that HONO elimination could occur, as the C1 and H2 nuclei had asymmetrically large electrophilic responses paired with H2 proximity to the O4 atom of a reactive axial nitro group. The nuclear Fukui function provided useful insight into the mechanistic effects of electronic perturbation in both the vapor phase and solid-state RDX. The concept of force derivative with respect to the electronic structure (eq 2) may be explored to use higher-order derivatives (e.g., with respect to both the electronic structure and nuclear position) for further understanding the solid-state reactions.

Acknowledgment. The research was supported by NSF (DMR-0449633). The authors would like to thank Dr. Shaoxin Feng for his technical support in this project.

References

(1) Tsiaousis, D.; Munn, R. W. Energy of charged states in the RDX crystal: Trapping of charge-transfer pairs as a possible mechanism for initiating detonation. *J. Chem. Phys.* **2005**, *122*, 184708.

(2) Luty, T.; Ordon, P.; Eckhardt, C. J. A model for mechanochemical transformations: Applications to molecular hardness, instabilities, and shock initiation of reaction. *J. Chem. Phys.* **2002**, *117*, 1775−1785.

(3) Ryzhkov, L. R.; Toscano, J. P. Crystal Lattice Effects on the Orientation and Orbital Degeneracy of Nitric Oxide Trapped in Nitramine Single Crystals. *Cryst. Growth Des.* **2005**, *5*, 2066−2072.

(4) Chakraborty, D.; Muller, R. P.; Dasgupta, S.; Goddard, W. A. The mechanism for unimolecular decomposition of RDX (1,3,5-trinitro-1,3,5-triazine), an ab initio study. *J. Phys. Chem. A* **2000**, *104*, 2261−2272.

(5) Zhao, X. S.; Hintsa, E. J.; Lee, Y. T. Infrared Multiphoton Dissociation of RDX in a Molecular-Beam. *J. Chem. Phys.* **1988**, *88*, 801−810.

(6) Behrens, R.; Bulusu, S. Thermal-Decomposition of Energetic Materials .3. Temporal Behaviors of the Rates of Formation of the Gaseous Pyrolysis Products from Condensed-Phase Decomposition of 1,3,5-Trinitrohexahydro-S-Triazine. *J. Phys. Chem.* **1992**, *96*, 8877−8891.

(7) Behrens, R.; Bulusu, S. Thermal-Decomposition of Energetic Materials .4. Deuterium-Isotope Effects and Isotopic Scrambling (H/D, C-13/O-18, N-14/N-15) in Condensed-Phase Decomposition of 1,3,5-Trinitrohexahydro-S-Triazine. *J. Phys. Chem.* **1992**, *96*, 8891−8897.

(8) Botcher, T. R.; Wight, C. A. Explosive Thermal-Decomposition Mechanism of RDX. *J. Phys. Chem.* **1994**, *98*, 5441−5444.

(9) Maharrey, S.; Behrens, R. Thermal decomposition of energetic materials. 5. Reaction processes of 1,3,5-trinitrohexahydro-s-triazine below its melting point. *J. Phys. Chem.* A **2005**, *109*, 11236−11249.

(10) Choi, M.; Kim, H.; Chung, C. FT-IR Spectra of Photochemical-Reaction Products of Crystalline RDX. *J. Phys. Chem.* **1995**, *99*, 15785−15789.

(11) Dremin, A. N. Shock Discontinuity Zone Effect - the Main Factor in the Explosive Decomposition Detonation Process. *Philos. Trans. R. Soc. London, Ser. A* **1992**, *339*, 355−364.

(12) Owens, F. J.; Sharma, J. X-Ray Photoelectron-Spectroscopy and Paramagnetic-Resonance Evidence for Shock-Induced Intramolecular Bond Breaking In Some Energetic Solids. *J. Appl. Phys.* **1979**, *51*, 1494.

(13) Pace, M. D. EPR-Spectra of Photochemical NO_2 Formation in Monocyclic Nitramines and Hexanitrohexaazaisowurtzitane. *J. Phys. Chem.* **1991**, *95*, 5858−5864.

(14) Gilman, J. J. *Chem. Propul. Inf. Agency* **1992**, *589*, 379.

(15) Gilman, J. J. Mechanochemistry. *Science* **1996**, *274*, 65.

(16) Chambers, G. P.; Lee, R. J.; Oxby, T. J.; Perger, W. F. *Shock Compression of Condensed Matter*; AIP Conf. Proc. No. 620, 2002, Melville.

(17) Ershov, A. P. Ionization During Detonation of Solid Explosives. *Combust. Expl. Shock Waves* **1975**, *11*, 798−803.

(18) Ershov, A. P.; Zubkov, P. I.; Lukyanchikov, L. A. Measurements of Electrical-Conductivity Profile in Detonation Front of Solid Explosives. *Combust. Expl. Shock Waves* **1974**, *10*, 776−782.

(19) Zubkov, P. I.; Lukyanch, La; Novoselo, Bs. Electrical-Conductivity in Detonation Zone of Condensed Explosives. *Combust. Expl. Shock Waves* **1971**, *7*, 253−256.

(20) Caulder, S. M.; Buess, M. L.; Garroway, A. N.; Miller, P. J. NQR Line Broadening Due to Crystal Lattice Imperfections and Its Relationship to Shock Sensitivity; Shock Compression of Condensed Matter - 2003: Proceedings of the Conference of the American Physical Society Topical Group on Shock Compression of Condensed Matter, 2004, Portland, Oregon, U.S.A.

(21) Kuklja, M. M. On the initiation of chemical reactions by electronic excitations in molecular solids. *Appl. Phys. A* **2003**, *76*, 359−366.

(22) Kuklja, M. M.; Aduev, B. P.; Aluker, E. D.; Krasheninin, V. I.; Krechetov, A. G.; Mitrofanov, A. Y. Role of electronic excitations in explosive decomposition of solids. *J. Appl. Phys.* **2001**, *89*, 4156−4166.

(23) Kuklja, M. M.; Kunz, A. B. Compression-induced effect on the electronic structure of cyclotrimethylene trinitramine containing an edge dislocation. *J. Appl. Phys.* **2000**, *87*, 2215−2218.

(24) Kuklja, M. M.; Stefanovich, E. V.; Kunz, A. B. An excitonic mechanism of detonation initiation in explosives. *J. Chem. Phys.* **2000**, *112*, 3417−3423.

(25) Haussuhl, S. Elastic and thermoelastic properties of selected organic crystals: acenaphthene, trans-azobenzene, benzophenone, tolane, trans-stilbene, dibenzyl, diphenyl sulfone, 2,2′-biphenol, urea, melamine, hexogen, succinimide, pentaerythritol, urotropine, malonic acid, dimethyl malonic acid, maleic acid, hippuric acid, aluminium acetylacetonate, iron acetylacetonate, and tetraphenyl silicon. *Z. Kristallogr.* **2001**, *216*, 339−353.

(26) Haycraft, J. J.; Stevens, L. L.; Eckhardt, C. J. The elastic constants and related properties of the energetic material cyclotrimethylene trinitramine (RDX) determined by Brillouin scattering. *J. Chem. Phys.* **2006**, *124*, 024712.

(27) Schwarz, R. B.; Hooks, D. E.; Dick, J. J.; Archuleta, J. I.; Martinez, A. R. Resonant ultrasound spectroscopy measurement of the elastic constants of cyclotrimethylene trinitramine. *J. Appl. Phys.* **2005**, *98*, 056106.

(28) Sewell, T. D. Monte Carlo calculations of the hydrostatic compression of hexahydro-1,3,5-trinitro-1,3,5-triazine and beta-octahydro-1,3,5,7-tetranitro-1,3,5,7-tetrazocine. *J. Appl. Phys.* **1998**, *83*, 4142−4145.

(29) Ye, S.; Tonokura, K.; Koshi, M. A Raman study of energy transfer processes between phonon and vibron in RDX and β-HMX at low temperatures. *Kayaku Gakkaishi* **2002**, *63*, 104.

(30) Boyd, S.; Gravelle, M.; Politzer, P. Nonreactive molecular dynamics force field for crystalline hexahydro-1,3,5-trinitro-1,3,5 triazine. *J. Chem. Phys.* **2006**, *124*, 104508.

(31) Harris, N. J.; Lammertsma, K. Ab initio density functional computations of conformations and bond dissociation energies for hexahydro-1,3,5-trinitro-1,3,5-triazine. *J. Am. Chem. Soc.* **1997**, *119*, 6583−6589.

(32) Rice, B. M.; Chabalowski, C. F. Ab initio and nonlocal density functional study of 1,3,5-trinitro-s-triazine (RDX) conformers. *J. Phys. Chem. A* **1997**, *101*, 8720−8726.

(33) Choi, C. S.; Prince, E. Crystal-Structure of Cyclotrimethylene-Trinitramine. *Acta Crystallogr. B* **1972**, *B28*, 2857−2862.

(34) Feng, S.; Li, T. Understanding solid-state reactions of organic crystals with density functional theory-based concepts. *J. Phys. Chem. A* **2005**, *109*, 7258−7263.

(35) Li, T.; Feng, S. Study of crystal packing on the solid-state reactivity of indomethacin with density functional theory. *Pharm. Res.* **2005**, *22*, 1964−1969.

(36) Hohenberg, P.; Kohn, W. Inhomogeneous Electron Gas. *Phys. Rev.* **1964**, *B136*, B864−B871.

(37) Kohn, W.; Becke, A. D.; Parr, R. G. Density functional theory of electronic structure. *J. Phys. Chem.* **1996**, *100*, 12974−12980.

(38) Parr, R. G.; Yang, W. T. Density-functional theory of the electronic structure of molecules. *Annu. Rev. Phys. Chem.* **1995**, *46*, 701−728.

(39) Feynman, R. P. Forces in Molecules. *Phys. Rev.* **1939**, *56*, 340.

(40) Hellmann, H. *Einführung in die Quantenchemie*; Deuticke: Vienna, 1937.

(41) Cohen, M. H.; Gandugliapirovano, M. V.; Kudrnovsky, J. Electronic and Nuclear-Chemical Reactivity. *J. Chem. Phys.* **1994**, *101*, 8988−8997.

(42) DeProft, F.; Liu, S. B.; Geerlings, P. Calculation of the Nuclear Fukui Function and New Relations for Nuclear Softness and Hardness Kernels. *J. Chem. Phys.* **1998**, *108*, 7549−7554.

(43) Balawender, R.; De, Proft, F.; Geerlings, P. Nuclear Fukui Function and Berlin's Binding Function: Prediction of the Jahn-Teller Distortion. *J. Chem. Phys.* **2001**, *114*, 4441−4449.

(44) Doll, K.; Saunders, V. R.; Harrison, N. M. Analytical Hartree-Fock gradients for periodic systems. *Int. J. Quantum Chem.* **2001**, *82*, 1−13.

CT600202E